

Time-Dependent Tilted Pulsed-Beams and Their Properties

Yakir Hadad and Timor Melamed

Abstract—Novel time-dependent wavepacket equation and its pulsed field solutions are obtained by utilizing a non-orthogonal coordinate system which is *a priori* matched to the field's planar linearly-delayed pulsed localized aperture distributions. These waveobjects that serve as the building blocks for various time-dependent beam-expansion schemes, are termed tilted pulsed-beams. Iso-axial pulsed-beams are parameterized in term of beam-widths, waist-locations, collimation-lengths, wave-front radii of curvature, and other features. Emphasis is placed on a direct time-domain derivation. A numerical example is presented in which the enhanced accuracy of the tilted pulsed-beams over the conventional (orthogonal coordinates) ones in the well-collimated zone is demonstrated.

Index Terms—Electromagnetic propagation, parabolic wave equation, pulsed beams.

I. INTRODUCTION

PARABOLIC wave equation (PWE) methods are a major tool for analysis and synthesis of scalar or electromagnetic fields [1]–[3]. Solutions of the PWE are subject to boundary conditions which are obtained by matching the field aperture distribution on a given surface to the PWE model. For problems in which the aperture distribution is given over a surface that is perpendicular to the initial paraxial direction, it may be conveniently matched to the PWE model.

PWE methods can be used for obtaining beam waveobjects that serve as the building blocks for several beam-type expansion schemes by utilizing the beam's mutual spectral and spatial localization. Locality considerations have been utilized for solving beam-type waveobjects propagation in generic media profiles such as inhomogeneous [4]–[7], anisotropic [8]–[15], for time-dependent pulsed-beams, in dispersive media [16]–[20] and for inverse scattering applications [21], [22].

Beam solutions are significant for beam-type (phase-space) expansions of scalar or electromagnetic fields such as Gabor-based expansions [23], [24], continuous spectrum representations [24]–[26] or for the frame-based field expansions [27]–[31]. Exact beam-type expansions require beam solutions that match localized aperture planar distributions. In these solutions the boundary plane over which the aperture

field distribution is given is generally *not perpendicular* to the beam-axis. Since such waveobjects serve as the basic building blocks for different pulsed beam expansions, it is an important task to parameterize them in order to calibrate these expansion schemes and utilize them in different scattering scenarios [32]–[41]

Recently, a novel time-harmonic PWE was obtained by applying a non-orthogonal coordinate system which is *a priori* matched to localized aperture field distributions [7], [42], [43]. Localized solutions to this equation that exactly match linearly-phased Gaussian aperture distributions were termed tilted Gaussian beams.

In the present contribution we extend these results and introduce in Section III a time-dependent wavepacket equation in non-orthogonal coordinates and derive in Section IV its localized field solutions that are termed *tilted pulsed-beams* (tilted PBs). The properties and parameterization of these waveobjects are explored in Section V as well as the additional wave phenomena associated with applying a non-orthogonal coordinate system. Finally in Section VI we present a numerical analysis of the accuracy of the tilted PBs in comparison to the conventional PBs and demonstrate that the tilted PBs are more accurate over a wide range of propagation regimes and parameters.

II. FORMULATION

We seek for *asymptotically-exact* PB solutions, $B(\mathbf{r}, t)$, to the 3D scalar wave equation

$$[\nabla^2 - v^{-2}\partial_t^2] B(\mathbf{r}, t) = 0, \quad \nabla^2 = \frac{\partial^2}{\partial x_1^2} + \frac{\partial^2}{\partial x_2^2} + \frac{\partial^2}{\partial z^2} \quad (1)$$

in the $z \geq 0$ half-space, where v denotes the medium wave-speed. Here $\mathbf{r} = (x_1, x_2, z)$ is the conventional Cartesian coordinate frame with $\mathbf{x} = (x_1, x_2)$ denoting the transverse coordinates.

A. Analytic Signals

In order to gain flexibility in the derivation, particularly when evanescent spectra are involved, it is convenient to use the analytic signal representation (more details are given in Sections V-A and V-B). Given a real signal $f(t)$ that is defined for real t , the corresponding analytic signal is defined by the convolution integral

$$\check{f}(t) = \frac{-1}{\pi j} \int_{-\infty}^{\infty} dt' \frac{f(t')}{t - t'}, \quad \text{Im}t \geq 0. \quad (2)$$

Manuscript received November 26, 2010; revised February 24, 2011; accepted March 14, 2011. Date of publication August 08, 2011; date of current version October 05, 2011.

The authors are with the Department of Electrical and Computer Engineering, Ben-Gurion University of the Negev, Beer Sheva 84105, Israel (e-mail: timormel@ee.bgu.ac.il).

Digital Object Identifier 10.1109/TAP.2011.2163784

Here and henceforth, analytic signals are denoted by a breve mark ($\check{\cdot}$). The limit of the analytic signal on the *real* t -axis is related to the *real* signal $f(t)$ by

$$\check{f}(t) = f(t) - j\mathcal{H}_t f(t), \quad t \text{ real} \quad (3)$$

where $\mathcal{H}_t = \mathcal{P}(1/\pi t) \otimes$ is the Hilbert transform operator, with \mathcal{P} denoting Cauchy's principal value and \otimes denoting a temporal convolution. Therefore the real signal for real t is recovered from the analytic signal via $f(t) = \text{Re}\check{f}(t)$. Alternatively the analytic signal $\check{f}(t)$ can be obtained by applying a one-sided (positive frequencies) inverse Fourier transform to the spectral (frequency domain) distribution of the real signal $f(t)$. Since this paper is concerned with a *direct* time-domain derivation, this approach is not investigated here.

B. Statement of the Problem

We are aimed at obtaining PB waveobjects that can serve as the building blocks for different time-dependent beam-type field expansion schemes. These expansion schemes decompose the field over a spatial-directional-temporal (spectral) lattice of spectral variables. The propagating elements are PBs that are identified by their planar aperture field distributions over the $z = 0$ plane, $B_0(\mathbf{x}, t)$, of the form [26], [28]

$$B_0(\mathbf{x}, t) = \text{Re}\check{f} \left[t - v^{-1} \left(\bar{\boldsymbol{\xi}}^T \mathbf{x} + \frac{1}{2} \mathbf{x}^T \boldsymbol{\Gamma}_0 \mathbf{x} \right) \right] \quad (4)$$

where $\bar{\boldsymbol{\xi}} = (\bar{\xi}_1, \bar{\xi}_2)$ are the expansion (directional) spectral variables. Throughout this work, all vectors are column vectors and superscript T denotes the matrix (or the vector) transpose, so that the linear delay-term in (4) reads $\bar{\boldsymbol{\xi}}^T \mathbf{x} = \bar{\xi}_1 x_1 + \bar{\xi}_2 x_2$. In (4), $\boldsymbol{\Gamma}_0$ is a 2×2 complex symmetric matrix with a negative definite imaginary part. Here and henceforth, bold lower-case letters are used to denote vectors, whereas bold capital letters are used to denote matrices. Note that (4) consists of a localized pulsed distribution with a quadratic delay term as well as a linear one that causes the beam to tilt with respect to the aperture $z = 0$ plane.

III. THE NON-ORTHOGONAL WAVEPACKET EQUATION

We apply here the *non-orthogonal local coordinate system* which was introduced in [42]. This system is *a priori* matched to the aperture field distribution in (4). The spectral variables

$$\bar{\boldsymbol{\xi}} = (\bar{\xi}_1, \bar{\xi}_2) = (\cos \vartheta_1, \cos \vartheta_2) \quad (5)$$

form a unit vector in the direction of the beam-axis

$$\hat{\mathbf{z}}_b = (\bar{\boldsymbol{\xi}}, \bar{\zeta}), \quad \bar{\zeta} = \sqrt{1 - \bar{\xi}_1^2 - \bar{\xi}_2^2} = \cos \vartheta_3 \quad (6)$$

where $\vartheta_{1,2,3}$ denote the beam-axis angles with the axes x_1 , x_2 and z (see Fig. 1). In this system, observation point $\mathbf{r} =$

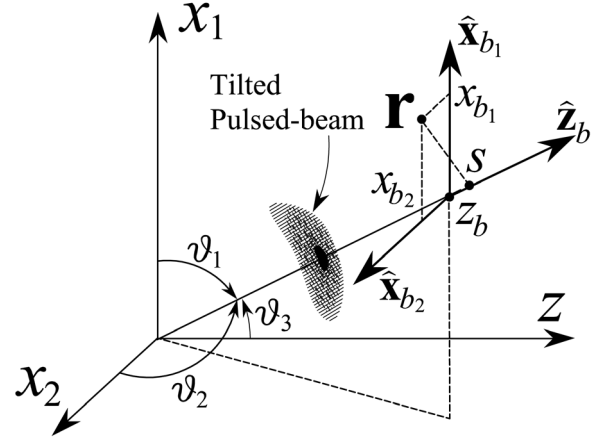


Fig. 1. Non-orthogonal local beam coordinate system. Observation point \mathbf{r} is described by the non-orthogonal system $\mathbf{r}_b = (x_{b_1}, x_{b_2}, z_b)$ in (7). The delay term in (9) is accumulated according to the (perpendicular) optic length (Eikonal) s .

(x_1, x_2, z) is represented by a local beam coordinates $\mathbf{r}_b = (x_{b_1}, x_{b_2}, z_b)$ which are defined by the transformation

$$\mathbf{r}_b = \begin{bmatrix} 1 & 0 & \frac{-\bar{\xi}_1}{\bar{\zeta}} \\ 0 & 1 & \frac{-\bar{\xi}_2}{\bar{\zeta}} \\ 0 & 0 & \bar{\zeta}^{-1} \end{bmatrix} \mathbf{r}, \quad \mathbf{r} = \begin{bmatrix} 1 & 0 & \bar{\xi}_1 \\ 0 & 1 & \bar{\xi}_2 \\ 0 & 0 & \bar{\zeta} \end{bmatrix} \mathbf{r}_b. \quad (7)$$

We denote $\hat{\mathbf{x}}_{b_1}$, $\hat{\mathbf{x}}_{b_2}$ and $\hat{\mathbf{z}}_b$ as the unit-vectors in the direction of the x_{b_1} , x_{b_2} and z_b axes, respectively. Note that $\hat{\mathbf{x}}_{b_1} = \hat{\mathbf{x}}_1$, $\hat{\mathbf{x}}_{b_2} = \hat{\mathbf{x}}_2$, whereas $\hat{\mathbf{z}}_b$ is given in (6). Here and henceforth, hat over a vector denotes a unit-vector.

In this system the transverse local beam coordinates, x_{b_1} and x_{b_2} , lie on a plane parallel to the aperture distribution plane at $z = 0$, whereas the longitudinal coordinate, z_b , is directed along the tilted beam-axis. Using these definitions, the z_b -axis is identified as the *paraxial* propagation direction, and the transverse coordinates, x_{b_1} and x_{b_2} , lie on a plane parallel to the (x_1, x_2) plane and are centered at the intersection of the (x_{b_1}, x_{b_2}) plane with the z_b -axis (see Fig. 1).

In order to obtain the wave equation in the non-orthogonal coordinates, we follow the time-harmonic derivation in [42] and evaluate the metric coefficients tensor of the transformation in (7) and insert it into the Laplacian operator in (1). The result is (see details in [42])

$$\begin{aligned} & (1 - \bar{\xi}_2^2) B_{x_{b_1} x_{b_1}} + (1 - \bar{\xi}_1^2) B_{x_{b_2} x_{b_2}} + 2\bar{\xi}_1 \bar{\xi}_2 B_{x_{b_1} x_{b_2}} \\ & - 2\bar{\xi}_1 B_{x_{b_1} z_b} - 2\bar{\xi}_2 B_{x_{b_2} z_b} + B_{z_b z_b} - v^{-2} \bar{\zeta}^2 B_{tt} = 0 \end{aligned} \quad (8)$$

where coordinate subscripts denote partial derivatives with respect to the coordinates, i.e., $B_{x_{b_1}} \equiv \partial B / \partial x_{b_1}$, $B_{tt} \equiv \partial^2 B / \partial t^2$, etc.

We are concerned with asymptotically evaluating the field $B(\mathbf{r}, t)$ that satisfies the 3D wave equation in (8) with boundary condition (4). High-frequency/short-pulsed wave-fields propagate along ray trajectories. Thus, solutions of the wave equation at some observation point \mathbf{r} close to the ray trajectory can be evaluated asymptotically by solving the PWE along the trajectory. By referring to boundary condition (4), we identify $\hat{\mathbf{z}}_b$ in (6) as the direction of the ray trajectory which emanates from

the aperture point $\mathbf{r} = (0, 0, 0)$. Therefore we assume here that the wave field has the following *short-pulsed* form

$$B(\mathbf{r}_b, t) = U(\mathbf{r}_b, t_s), \quad t_s(\mathbf{r}_b, t) = t - v^{-1}s(\mathbf{r}_b) \quad (9)$$

where the Eikonal

$$s(\mathbf{r}_b) = z_b + \bar{\xi}_1 x_{b_1} + \bar{\xi}_2 x_{b_2} \quad (10)$$

is the projection of the observation vector \mathbf{r} on the direction of the beam-axis z_b . Using the ray-field (9)–(10), we can evaluate the derivatives in (8)

$$\begin{aligned} B_{x_{b_1}} &= [U_{x_{b_1}} - v^{-1}\bar{\xi}_1 U_{t_s}], \\ B_{x_{b_1}x_{b_1}} &= [U_{x_{b_1}x_{b_1}} - 2v^{-1}\bar{\xi}_1 U_{x_{b_1}t_s} + v^{-2}\bar{\xi}_1^2 U_{t_s t_s}] \end{aligned} \quad (11)$$

and so-forth for all partial derivatives in (8). In (11) all partial derivatives of $U(\mathbf{r}_b, t_s) = U(x_{b_1}, x_{b_2}, z_b, t_s)$ are taken with respect to the corresponding argument, i.e., prior to sampling at $t_s = t - v^{-1}s(\mathbf{r}_b)$.

Next, following conventional paraxial ray-theory [3]–[5], we assume that

$$v^{-1}|U_{t_s}| \gg |U_{z_b}|. \quad (12)$$

By inserting (11) as well as all the other partial derivatives into (8) and neglecting terms according to (12), the wave equation is approximated by

$$\begin{aligned} (1 - \bar{\xi}_2^2) U_{x_{b_1}x_{b_1}} + 2\bar{\xi}_1\bar{\xi}_2 U_{x_{b_1}x_{b_2}} \\ + (1 - \bar{\xi}_1^2) U_{x_{b_2}x_{b_2}} - 2v^{-1}\bar{\zeta}^2 U_{z_b t_s} = 0. \end{aligned} \quad (13)$$

Equation (13) is termed here the *Non-orthogonal Wavepacket Equation* (NOWE). Note that by setting $\vartheta_1 = \vartheta_2 = \pi/2$ (namely $\bar{\xi}_1 = \bar{\xi}_2 = 0$) in (13), the NOWE reduces to the well-known wavepacket equation in orthogonal coordinates [5].

IV. TILTED PBS

Tilted PBs that are defined by aperture distributions of linearly-delated pulsed windows of the form in (4) are of highly significance as they serve as the building blocks for time-dependent beam-type expansions [26], [28]. In this section, we obtain asymptotically-exact expressions for these wavepackets.

In view of the aperture field distribution in (4), we are seeking localized beam solutions of the NOWE and assume a beam-type field of the form

$$U(\mathbf{r}_b, t_s) = \text{Re} \left\{ A(z_b) \check{f} \left[t_s - v^{-1} \frac{1}{2} \mathbf{x}_b^T \mathbf{\Gamma}(z_b) \mathbf{x}_b \right] \right\} \quad (14)$$

where $\mathbf{x}_b = (x_{b_1}, x_{b_2})$, $A(z_b)$ denotes a complex amplitude and the so-called complex curvature matrix $\mathbf{\Gamma}$ is a complex symmetrical matrix with Γ_{ij} denoting its (i, j) th element so that the argument in (14) is of the quadratic form $\mathbf{x}_b^T \mathbf{\Gamma} \mathbf{x}_b = x_{b_1}^2 \Gamma_{11} + 2x_{b_1}x_{b_2} \Gamma_{12} + x_{b_2}^2 \Gamma_{22}$. The matrix $\mathbf{\Gamma}$ has a negative definite imaginary part, hence beam-field (14) exhibits a decay away from the beam-axis. Pulsed beam-fields of the form in (14), which carry aperture localized pulsed distributions over the tilted $z_b = 0$ plane, are termed here *tilted PBs*.

Next, we insert the PB form in (14) into the NOWE (13). By setting the coefficients of the temporal derivatives \check{f}' and \check{f}'' to

zero for all observation points, we obtain two vector equations. The first equation is a vector Riccati-type equation for $\mathbf{\Gamma}(z_b)$,

$$\begin{aligned} \mathbf{\Gamma}(z_b) \mathbf{\Psi} \mathbf{\Gamma}(z_b) + \bar{\zeta}^2 \mathbf{\Gamma}'(z_b) = 0, \\ \mathbf{\Psi} = \begin{bmatrix} (1 - \bar{\xi}_2^2) & \bar{\xi}_1 \bar{\xi}_2 \\ \bar{\xi}_1 \bar{\xi}_2 & (1 - \bar{\xi}_1^2) \end{bmatrix} \end{aligned} \quad (15)$$

whereas the second equation,

$$\text{trace}[\mathbf{\Psi} \mathbf{\Gamma}(z_b)] A(z_b) + 2\bar{\zeta}^2 A'(z_b) = 0 \quad (16)$$

serves as the amplitude $A(z_b)$ once the Riccati equation in (15) is solved. In (15)–(16) the prime denotes a derivative with respect to the argument.

The solution of the Riccati equation is [42]

$$\mathbf{\Gamma}(z_b) = [\mathbf{\Gamma}_0^{-1} + \bar{\zeta}^{-2} \mathbf{\Psi} z_b]^{-1} \quad (17)$$

where $\mathbf{\Gamma}_0$ is the complex curvature matrix of the aperture field distribution over the $z_b = 0$ plane in (4). The beam amplitude, $A(z_b)$, is found by inserting (17) into (16). Using a straightforward separation of variables we obtain

$$A(z_b) = \sqrt{\frac{\det \mathbf{\Gamma}(z_b)}{\det \mathbf{\Gamma}_0}}. \quad (18)$$

The tilted PB can be written explicitly by using (17) and (18) in (14), and inserting into (9), which yields $B(\mathbf{r}_b, t) = \text{Re} \check{B}(\mathbf{r}_b, t)$ where

$$\check{B}(\mathbf{r}_b, t) = \sqrt{\frac{\det \mathbf{\Gamma}(z_b)}{\det \mathbf{\Gamma}_0}} \check{f}[t - \tau(\mathbf{r}_b)] \quad (19)$$

where

$$\tau(\mathbf{r}_b) = v^{-1} \left[s(\mathbf{r}_b) + \frac{1}{2} \mathbf{x}_b^T \mathbf{\Gamma}(z_b) \mathbf{x}_b \right] \quad (20)$$

s is given in (10) and $\mathbf{\Gamma}(z_b)$ is given in (17). Note that PB (19) satisfies the aperture field distribution in (4) exactly. This type of PB waveobjects exhibits frequency-independent collimation (Rayleigh) distance and therefore have been termed *iso-diffracting* [44]. The iso-diffracting feature makes these waveobjects highly suitable for UWB radiation representations [25], [27], [28], [45], [46].

V. PARAMETERIZATION OF THE TILTED PB

A. On-Axis Properties

The tilted PB in (19) propagates along the beam-axis that is defined for a given spectral-variable $\bar{\xi}$ by $\mathbf{x}_b = 0$, i.e., $x_{1,2} = z_b \bar{\zeta}^{-1} \bar{\xi}_{1,2}$. By separating the field's amplitude in (18) into its real and imaginary parts,

$$\sqrt{\frac{\det \mathbf{\Gamma}(z_b)}{\det \mathbf{\Gamma}_0}} = \gamma_r(z_b) + j\gamma_j(z_b) \quad (21)$$

and using the analytic signal limit for real t in (3) the *on-axis* PB field, $B(\mathbf{r}_b, t)|_{\mathbf{x}_b=0}$, is given by

$$B(z_b, t) = \gamma_r f(t - v^{-1}z_b) + \gamma_j \mathcal{H}_t f(t - v^{-1}z_b) \quad (22)$$

where $\mathcal{H}_t f(t)$ denotes the Hilbert transform of $f(t)$. Thus, the *on-axis* field is composed of a weighting of $f(t)$ and its Hilbert transform.

Since, according to (17), the real part of $\mathbf{\Gamma}^{-1}(z_b)$ increases linearly with z_b whereas its imaginary part remains constant, the weighting in the far-field (where z_b is large on the scale of the collimation-lengths) is made according to the real and imaginary parts of $1/\sqrt{\det \mathbf{\Gamma}_0}$. In the special case of an *imaginary* aperture curvature matrix where $\det \mathbf{\Gamma}_0$ is real and negative, for large z_b values $\gamma_r(z_b) \rightarrow 0$ so that the PB on-axis temporal shape undergoes a full Hilbert transform from $\gamma_r f(t)$ in the near-field to $\gamma_j \mathcal{H}_t f(t)$ in the far-field. The temporal, as well as the spatial off-axis features of the propagating PB in (19), depends on the specific choice of the pulse shape $f(t)$ and of the aperture complex curvature matrix, $\mathbf{\Gamma}_0$.

B. Lorentzian Temporal Dependence

A simple Lorentzian time-dependent pulse-shape is attained by choosing the analytic signal

$$\check{f}(t) = \check{\delta} \left(t + \frac{j}{2}T \right), \quad T > 0 \quad (23)$$

where T is a real parameter which models the time-dependent signal's temporal pulse length and $\check{\delta}(t)$ is the analytic delta-function in the upper half of the complex t -plane

$$\check{\delta}(t) = -(j\pi t)^{-1}, \quad \text{Im}t > 0. \quad (24)$$

For this pulse-shape the quadratic-Lorentzian aperture field distribution in (4) is given by

$$B_0(\mathbf{x}, t) = \text{Re} \check{\delta} \left[t + \frac{j}{2}T - v^{-1} \left(\bar{\boldsymbol{\xi}}^T \mathbf{x} + \frac{1}{2} \mathbf{x}^T \mathbf{\Gamma}_0 \mathbf{x} \right) \right]. \quad (25)$$

The tilted PB field in the $z \geq 0$ half space is given by $B(\mathbf{r}_b, t) = \text{Re} \check{B}(\mathbf{r}_b, t)$ where

$$\check{B}(\mathbf{r}_b, t) = \sqrt{\frac{\det \mathbf{\Gamma}(z_b)}{\det \mathbf{\Gamma}_0}} \check{\delta} \left[t + \frac{j}{2}T - \tau(\mathbf{r}_b) \right] \quad (26)$$

and τ is given in (20).

C. Off-Axis Parameterization

We now proceed to examine the properties of the Lorentzian tilted PB in (26) for *iso-axial* waveobjects. This family of PBs is used for expanding some aperture field using radially-symmetric windows (the parameterization of other tilted PBs can be

obtained in a similar manner). The Iso-axial GBs are characterized by a diagonal aperture complex curvature matrix of the form [26], [27], [29]

$$\mathbf{\Gamma}_0 = \mathbf{\Pi} \mathbf{\Gamma}_0, \quad \mathbf{\Gamma}_0 = (-Z + jF)^{-1}, \quad F > 0 \quad (27)$$

where Z and F are real parameters.

1) *Diagonalization of the Transverse Coordinates*: The real and imaginary parts of the complex iso-axial curvature matrix can be diagonalized simultaneously by rotating the \mathbf{x}_b -axes over constant z_b -planes by a z_b -independent angle Φ_c .

$$\tan 2\Phi_c = 2\bar{\xi}_1 \bar{\xi}_2 / (\bar{\xi}_1^2 - \bar{\xi}_2^2). \quad (28)$$

Therefore we define new (rotated) transversal coordinates \mathbf{x}_c which are obtained from \mathbf{x}_b via

$$\mathbf{x}_c = \mathbf{T}_c \mathbf{x}_b, \quad \mathbf{T}_c = \begin{bmatrix} \cos \Phi_c & \sin \Phi_c \\ -\sin \Phi_c & \cos \Phi_c \end{bmatrix}. \quad (29)$$

Angle Φ_c is identified as the angle between the x_1 -axis and the projection of the z_b -axis on (x_1, x_2) plane. By inserting (29) with (28) into (17), the quadratic phase in (20) is given by

$$\mathbf{x}_b^T \mathbf{\Gamma}(z_b) \mathbf{x}_b = \mathbf{x}_c^T \mathbf{\Gamma}_c(z_b) \mathbf{x}_c, \quad \mathbf{\Gamma}_c = \mathbf{T}_c \mathbf{\Gamma} \mathbf{T}_c^{-1}. \quad (30)$$

By inserting Φ_c in (28) into (30) with (27) and (17), we find that $\mathbf{\Gamma}_c$ takes the form of the *diagonal* matrix

$$\mathbf{\Gamma}_c(z_b) = \begin{bmatrix} (z_b \bar{\xi}^{-2} - Z + jF)^{-1} & 0 \\ 0 & (z_b - Z + jF)^{-1} \end{bmatrix} \quad (31)$$

for which Z and F are given in (27).

In order to parameterize the iso-axial tilted PB field, we separate the diagonalized complex curvature matrix $\mathbf{\Gamma}_c(z_b)$ into its real and imaginary parts by denoting

$$\text{Re} \mathbf{\Gamma}_c = \mathbf{L}_c^{-1}(z_b), \quad \text{Im} \mathbf{\Gamma}_c = -\mathbf{I}_c^{-1}(z_b). \quad (32)$$

Then using (31), we obtain

$$\mathbf{L}_c(z_b) = \begin{bmatrix} \bar{\xi}^{-2} \left[(z_b - Z_1) + \frac{F_1^2}{(z_b - Z_1)} \right] & 0 \\ 0 & (z_b - Z_2) + \frac{F_2^2}{(z_b - Z_2)} \end{bmatrix}$$

and

$$\mathbf{I}_c(z_b) = \begin{bmatrix} F \left[1 + \frac{(z_b - Z_1)^2}{F_1^2} \right] & 0 \\ 0 & F \left[1 + \frac{(z_b - Z_2)^2}{F_2^2} \right] \end{bmatrix} \quad (34)$$

with

$$Z_1 = Z \bar{\xi}^2, \quad Z_2 = Z, \quad F_1 = F \bar{\xi}^2, \quad F_2 = F. \quad (35)$$

Finally we separate $\tau(\mathbf{r}_b)$ in (20) into its real and imaginary parts

$$\tau(\mathbf{r}_b) = t_p(\mathbf{r}_b) - \left(\frac{j}{2}\right) T_p(\mathbf{r}_b) \quad (36)$$

where, using (30) and (32) in (20), we identify

$$t_p(\mathbf{r}_b) = v^{-1} \left(s + \frac{1}{2} \mathbf{x}_c^T \mathbf{L}_c^{-1} \mathbf{x}_c \right) \quad (37)$$

and

$$T_p(\mathbf{r}_b) = v^{-1} \mathbf{x}_c^T \mathbf{I}_c^{-1} \mathbf{x}_c \quad (38)$$

where \mathbf{L}_c and \mathbf{I}_c are given in (33) and (34), respectively.

The *real* Lorentzian wave-forms are given by

$$f(\mathbf{r}_b, t) = \frac{1}{\pi} \frac{(T_p + T)/2}{(t - t_p)^2 + (T_p + T)^2/4} \quad (39)$$

and

$$\mathcal{H}_t f(\mathbf{r}_b, t) = \frac{-1}{\pi} \frac{t - t_p}{(t - t_p)^2 + (T_p + T)^2/4} \quad (40)$$

where t_p and T_p are given in (37) and (38), respectively. The (real) tilted PB in (26) is obtained by weighting of the wave-forms in (39) and (40) as in (22), i.e.,

$$B(\mathbf{r}_b, t) = \gamma_r f(\mathbf{r}_b, t) + \gamma_j \mathcal{H}_t f(\mathbf{r}_b, t). \quad (41)$$

2) *Transversal Beam-Widths and Diffraction Angles*: By using (36) in (37) or (38), one can readily identify $t_p(\mathbf{r}_b)$ as the *paraxial propagation delay* along the z_b axis. For a given observation point \mathbf{r} , the beam field in (39) peaks at $t = t_p(\mathbf{r}_b)$ and its half-amplitude pulse-length and peak-value are given by $T/2$ and $2/\pi T$, respectively. The transverse half-amplitude *beam widths* of the tilted PB propagator in the (\mathbf{x}_c, z_b) principle planes, $W_{1,2}$, is obtained by solving $T_p(\mathbf{r}_b) + T = 2[T_p(0) + T]$. Note that the perpendicular beam width in the direction of the projection of x_{c1} is obtained by multiplying the x_{c1} -width by $\bar{\zeta}$ (cf. Fig. 2). This procedure yields

$$W_{1,2}(z_b) = 2\sqrt{vTF_{1,2} \left[1 + \frac{(z_b - Z_{1,2})^2}{F_{1,2}^2} \right]} \quad (42)$$

where $F_{1,2}$ and $Z_{1,2}$ are given in (35). Using (42) we identify $F_{1,2}$ as the *collimation-lengths* and $Z_{1,2}$ as the *waist-locations* with corresponding minimal beam-widths of $D_{1,2} = 2\sqrt{vTF_{1,2}}$ at the waists. Note that according to (42), near the waists where $|z_b - Z_{1,2}| \ll F_{1,2}$, the beam remains collimated

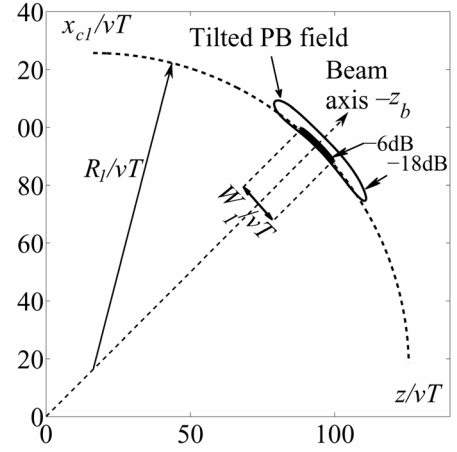


Fig. 2. Parameterization of the iso-axial tilted PB. The field is sampled over the (x_{c1}, z) plane for the Lorentzian time-dependence in (23). All parameters are normalized with respect to vT .

whereas far from the waists the beam spreads in constant diffraction angles of

$$\Theta_{1,2} = 2\sqrt{\frac{vT}{F_{1,2}}} \quad (43)$$

in the $(x_{c1,2}, z_b)$ planes.

3) *Phase-Front Radii of Curvature*: In order to parameterize the paraxial wavefront delay phenomenology as prescribed by the field quadratic delay-term $v^{-1}(1/2)\mathbf{x}_b^T \text{Re}\mathbf{\Gamma}(z_b)\mathbf{x}_b$ in *non-orthogonal* coordinates, the tilted PB is casted in the *paraxial geometrical optics* ray-field canonical form in *orthogonal* coordinates. This procedure has been introduced in [43]. We refer the reader to the results there in which the wave front radii of curvature are given by (43).

VI. NUMERICAL EXAMPLE

A. Parameterization

In order to verify the accuracy of the tilted PB parameterization we present in Fig. 2 the contour lines of -6 dB and -18 dB from the on-axis peak value of a PB field with a Lorentzian time-dependence. The field is sampled over the (x_{c1}, z) plane with field parameters of $\bar{\zeta} = \sqrt{2}/2$, $Z = 200vT$ and $F = 100vT$. The peak on-axis point was set to 0.65 of the collimation length away from the waist locations at $z_b = Z_1$ (i.e., $z_b = Z_1 + 0.65F_1$) so that the field is sampled at $t = 132T$. The corresponding wavefront radius of curvature in Section V-C-III is $R_1 = 110vT$, and the transverse -6 dB beam width in (42) is $W_1 = 15.5vT$. One can identify in Fig. 2 that the *numerically* evaluated -6 dB contour line agrees with the *theoretically* evaluated beam width and the wave front radius of curvature.

B. Accuracy Analysis

In this section we compare the accuracy of the tilted PBs with the convectional paraxial PBs which are given in local beam orthogonal coordinates. The reference solution is evaluated using a transient plane-wave spectral integration of the aperture field in (4).

1) *Tilted PBs*: The tilted PBs are given by (26) with the iso-axial curvature matrix in (31).

2) *Conventional PBs*: The convectional paraxial PB that are corresponding to the aperture field in (4) with the iso-axial aperture curvature in (27) are obtained by utilizing the local orthogonal beam-coordinates, $\mathbf{r}_o = (x_o, y_o, z_o)$, which are defined for a given spectral variables $\bar{\xi}$, by the rotation transformation $\mathbf{r}_o(\mathbf{r}) = \mathbf{T}_o \mathbf{r}$ where the rotation matrix \mathbf{T}_o is given by [26]

$$\mathbf{T}_o = \begin{bmatrix} \cot \vartheta_3 \cos \vartheta_1 & \cot \vartheta_3 \cos \vartheta_2 & -\sin \vartheta_3 \\ -\cos \vartheta_2 / \cos \vartheta_3 & \cos \vartheta_1 / \cos \vartheta_3 & 0 \\ \cos \vartheta_1 & \cos \vartheta_2 & \cos \vartheta_3 \end{bmatrix}. \quad (44)$$

Here $\vartheta_{1,2,3}$ are the spherical angles that define the beam-axis $\hat{\mathbf{z}}_b$ in (6). The conventional PBs for the Lorentzian time-dependence in (23) are given by $B_{Conv}(\mathbf{r}, t) = \text{Re} \check{B}_{Conv}(\mathbf{r}, t)$ where [26]

$$\check{B}_{Conv}(\mathbf{r}, t) = \sqrt{\frac{\det \mathbf{\Gamma}_o(z_o)}{\det \mathbf{\Gamma}_o(0)}} \delta \left[t + j \frac{1}{2} T - \tau_o(\mathbf{r}_o) \right] \quad (45)$$

where

$$\tau_o(\mathbf{r}_o) = v^{-1} \left[z_o + \frac{1}{2} \mathbf{x}_o^T \mathbf{\Gamma}_o(z_o) \mathbf{x}_o \right] \quad (46)$$

and $\mathbf{\Gamma}_o$ is given by

$$\mathbf{\Gamma}_o(z_o) = \begin{bmatrix} [z_o + (-Z + jF)\bar{\zeta}^2]^{-1} & 0 \\ 0 & (z_o - Z + jF)^{-1} \end{bmatrix} \quad (47)$$

for which Z and F are given in (27).

3) *Reference Solution*: The reference solution is evaluated using a transient plane-wave integration. The spectral representation of the aperture distribution in (4) with the iso-axial curvature in (27) and the Lorentzian time-dependence in (23) is given by [26]

$$\check{B}_{Ref}(\mathbf{r}, t) = \frac{1}{2\pi v \Gamma_0} \int_{-\infty}^{\infty} d^2 \xi \delta' \left[t + j \frac{1}{2} T - \tilde{\tau}(\xi) \right] \quad (48)$$

$$\tilde{\tau}(\xi) = v^{-1} \left[\xi \cdot \mathbf{x} + \zeta z - (2\Gamma_0)^{-1} (\xi - \bar{\xi}) \cdot (\xi - \bar{\xi}) \right]$$

where $\xi = (\xi_1, \xi_2)$ are the plane-wave (directional) spectral variables, $\xi = \sqrt{\xi_1^2 + \xi_2^2}$, and $\zeta = \sqrt{1 - \xi^2}$ denotes the longitudinal spectral normalized wavenumber with $\text{Re} \zeta \geq 0$ and $\text{Im} \zeta \leq 0$. In (48), $\delta'(t)$ denotes the derivative of the analytic delta-function in (24), i.e.,

$$\delta'(t) = \frac{1}{(j\pi t^2)}, \quad \text{Im} t > 0. \quad (49)$$

4) *Error Comparison*: In this section we compare the accuracy of the tilted PB in (26) (which is denoted here as $B_{Tilt}(\mathbf{r}, t)$) to the accuracy of the conventional PB in (45), $B_{Conv}(\mathbf{r}, t)$, both with respect the reference solution $B_{Ref}(\mathbf{r}, t)$. The 3D fields are evaluated over (x, z) plane for $\vartheta_2 = 0$ and for various values of ϑ_3 (various tilting) and z_b . We quantify the accuracy by the \mathbb{L}_1 norm of the difference of the PB and the reference PB over -3 dB domain where either

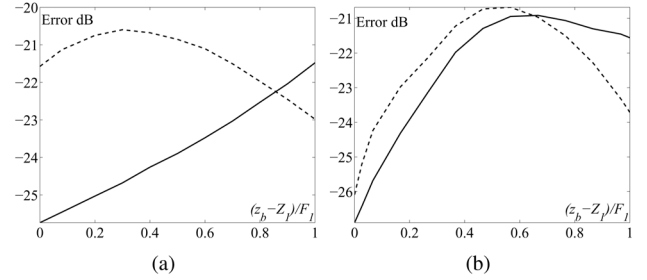


Fig. 3. Error of the tilted PBs (solid line) and conventional PBs (dashed line) with respect to the reference solution. The field parameters are $vT = 10^{-3}$, $Z = 0$, $F = 5vT$. The sampling time is set so that the PB is centered on various locations along the beam-axis z_b . The z_b -location in the horizontal axis is normalized with respect to the collimation length F_1 , i.e., $(z_b - Z)/F_1$. (a) $\vartheta_3 = 30^\circ$, (b) $\vartheta_3 = 60^\circ$.

the PB or the reference PB exceeds half of the reference PB's (absolute) maximum. This domain over (x, z) plane is denoted by Ω . Thus the relative error is

$$E_{Rel} = S^{-1} \int_{(x,z) \in \Omega} \frac{|B(x, z, t) - B_{Ref}(x, z, t)|}{|B_{Ref}(x, z, t)|} dx dz \quad (50)$$

where B denotes either the tilted PB or the conventional one and S is the area of Ω .

The relative errors in dB as a function of the z_b -location for $\vartheta_3 = 30^\circ, 60^\circ$ in (5) are plotted in Fig. 3(a) and (b), respectively. In these figures the *tilted* PB errors are plotted in solid lines and the *conventional* PB errors are plotted in dashed lines. The field parameters are $vT = 10^{-3}$, $Z = 0$, $F = 5vT$. The sampling time is set so that the PB is centered on various locations along the beam-axis z_b . The location is normalized with respect to the collimation length F_1 in (35), so that the well-collimated regime is characterized by $(z_b - Z_1)/F_1 \ll 1$ (see (42)). This figure demonstrates that the tilted PB exhibits an about 3–4 dB enhanced accuracy in the collimation range for $\vartheta_3 = 30^\circ$. The error difference decreases as the departure angle becomes perpendicular and for 60° the error difference reduces to about 1–1.5 dB.

Note that the error of the asymptotic solutions is quite small (less than -20 dB). Nevertheless, the PBs are the building blocks of the phase-space beam summation method (as described in Sections I and II-B). Thus, the overall error which is accumulated in the summation over the entire 5D spatial-directional-temporal spectral lattice is significantly higher than the accuracy of a single PB. Taking this into account, the 3–4 dB enhanced accuracy can be regarded as significant. Furthermore, beam-type expansions are usually tuned such that the scattering of a single spectral PB occurs in the well-collimated zone where the tilted PBs exhibit an enhanced accuracy. It should be noted though that in some practical applications the choice of F_1 is a tradeoff between collimation and spatial localization in relation to the size of the details in the medium [47], [48].

In order to evaluate the error for well collimated PBs we plot in Fig. 4 the errors as in Fig. 3 with $vT = 10^{-3}$, $Z = 0$ and $\vartheta_3 = 15^\circ$ for $F = 150vT, 1500vT$ in Fig. 4(a) and (b), respectively. By inserting $F = 150$ and $F = 1500$ into (43), we evaluate the corresponding diffraction angles to be $\Theta = 0.6$ and 0.2 radians, respectively. Here the tilted PB exhibits an enhanced

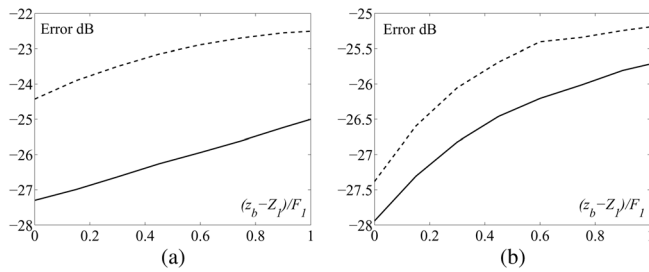


Fig. 4. Same as Fig. 3 with $\vartheta_3 = 15^\circ$ for (a) $F = 150vT$, (b) $F = 1500vT$.

accuracy of about 3 dB for $F = 150vT$ and a smaller improvement of 0.7 dB for $F = 1500vT$. The figures demonstrate the enhanced accuracy of the tilted PBs over the conventional ones for a wide range of parameters while the computational complexity remains exactly the same.

VII. CONCLUDING REMARKS

Novel time-dependent beam-type waveobjects were introduced and termed tilted PBs. These 3D wavepackets are paraxial solutions of the time-dependent wave equation in non-orthogonal coordinates that are *a priori* matched to pulsed localized aperture distributions. Parametrization of tilted PBs in homogeneous media was carried out. The waveobjects were parameterized in terms of waist-locations, beam-widths, collimation-lengths, and other wave features. A numerical example was presented which demonstrated the enhanced accuracy of the tilted PBs over the conventional ones in the well-collimated zone.

REFERENCES

- [1] S. N. Vlasov and V. I. Talanov, "The parabolic equation in the theory of wave propagation," *Radiophys. Quantum Electron.*, vol. 38, pp. 1–12, 1995.
- [2] M. Levys, *Parabolic Equation Methods for Electromagnetic Wave Propagation*. London, U.K.: Inst. Elect. Eng., 2000.
- [3] C. Chapman, *Fundamentals of Seismic Wave Propagation*. Cambridge, UK: Cambridge Univ. Press, 2004.
- [4] V. Červený, M. M. Popov, and I. Pšenčík, "Computation of wave fields in inhomogeneous media—Gaussian beam approach," *Geophys. J. Roy. Astron. Soc.*, vol. 70, pp. 109–128, 1982.
- [5] E. Heyman, "Pulsed beam propagation in an inhomogeneous medium," *IEEE Trans. Antennas Propag.*, vol. 42, pp. 311–319, 1994.
- [6] T. Melamed, "Phase-space Green's functions for modeling time-harmonic scattering from smooth inhomogeneous objects," *J. Math. Phys.*, vol. 45, pp. 2232–2246, 2004.
- [7] Y. Hadad and T. Melamed, "Tilted Gaussian beam propagation in inhomogeneous media," *J. Opt. Soc. Am. A*, vol. 27, pp. 1840–1850, 2010.
- [8] S. Y. Shin and L. B. Felsen, "Gaussian beams in anisotropic media," *Appl. Phys.*, vol. 5, pp. 239–250, 1974.
- [9] R. Simon, "Anisotropic Gaussian beams," *Opt. Commun.*, vol. 46, pp. 265–269, 1983.
- [10] R. Simon and N. Mukunda, "Shape-invariant anisotropic Gaussian Schell-model beams: A complete characterization," *J. Opt. Soc. Am. A*, vol. 15, pp. 1361–1370, 1998.
- [11] E. Poli, G. V. Pereverzev, and A. G. Peeters, "Paraxial Gaussian wave beam propagation in an anisotropic inhomogeneous plasma," *Phys. Plasmas*, vol. 6, pp. 5–11, Jan. 1999.
- [12] L. I. Perez and M. T. Garea, "Propagation of 2D and 3D Gaussian beams in an anisotropic uniaxial medium: Vectorial and scalar treatment," *Optik*, vol. 111, pp. 297–306, 2000.
- [13] I. Tinkelman and T. Melamed, "Gaussian beam propagation in generic anisotropic wavenumber profiles," *Opt. Lett.*, vol. 28, pp. 1081–1083, 2003.
- [14] I. Tinkelman and T. Melamed, "Local spectrum analysis of field propagation in anisotropic media, Part I—Time-harmonic fields," *J. Opt. Soc. Am. A*, vol. 22, pp. 1200–1207, 2005.
- [15] I. Tinkelman and T. Melamed, "Local spectrum analysis of field propagation in anisotropic media, Part II—Time-dependent fields," *J. Opt. Soc. Am. A*, vol. 22, pp. 1208–1215, 2005.
- [16] A. G. Khatkevich, "Propagation of pulses and wave packets in dispersive gyrotropic crystals," *J. Appl. Spectrosc.*, vol. 46, pp. 203–207, 1987.
- [17] T. Melamed and L. B. Felsen, "Pulsed beam propagation in lossless dispersive media, Part I: Theory," *J. Opt. Soc. Am. A*, vol. 15, pp. 1268–1276, 1998.
- [18] T. Melamed and L. B. Felsen, "Pulsed beam propagation in lossless dispersive media, Part II: A numerical example," *J. Opt. Soc. Am. A*, vol. 15, pp. 1277–1284, 1998.
- [19] T. Melamed and L. B. Felsen, "Pulsed beam propagation in dispersive media via pulsed plane wave spectral decomposition," *IEEE Trans. Antennas Propag.*, vol. 48, pp. 901–908, 2000.
- [20] A. P. Kiselev, "Localized light waves: Paraxial and exact solutions of the wave equation (a review)," *Opt. Spectrosc.*, vol. 102, pp. 603–622, 2007.
- [21] T. Melamed, E. Heyman, and L. B. Felsen, "Local spectral analysis of short-pulse-excited scattering from weakly inhomogeneous media: Part I—forward scattering," *IEEE Trans. Antennas Propag.*, vol. 47, pp. 1208–1217, 1999.
- [22] T. Melamed, E. Heyman, and L. B. Felsen, "Local spectral analysis of short-pulse-excited scattering from weakly inhomogeneous media: Part II—inverse scattering," *IEEE Trans. Antennas Propag.*, vol. 47, pp. 1218–1227, 1999.
- [23] J. J. Maciel and L. B. Felsen, "Systematic study of fields due to extended apertures by Gaussian beam discretization," *IEEE Trans. Antennas Propag.*, vol. 37, pp. 884–892, 1989.
- [24] B. Z. Steinberg, E. Heyman, and L. B. Felsen, "Phase space beam summation for time-harmonic radiation from large apertures," *J. Opt. Soc. Am. A*, vol. 8, pp. 41–59, 1991.
- [25] B. Z. Steinberg, E. Heyman, and L. B. Felsen, "Phase space beam summation for time dependent radiation from large apertures: Continuous parametrization," *J. Opt. Soc. Am. A*, vol. 8, pp. 943–958, 1991.
- [26] T. Melamed, "Phase-space beam summation: A local spectrum analysis for time-dependent radiation," *J. Electromag. Waves Appl.*, vol. 11, pp. 739–773, 1997.
- [27] A. Shlivinski, E. Heyman, A. Boag, and C. Letrou, "A phase-space beam summation formulation for ultra wideband radiation," *IEEE Trans. Antennas Propag.*, vol. 52, pp. 2042–2056, 2004.
- [28] A. Shlivinski, E. Heyman, and A. Boag, "A pulsed beam summation formulation for short pulse radiation based on windowed Radon transform (WRT) frames," *IEEE Trans. Antennas Propag.*, vol. 53, pp. 3030–3048, 2005.
- [29] T. Melamed, "Exact Gaussian beam expansion of time-harmonic electromagnetic waves," *J. Electromag. Waves Appl.*, vol. 23, pp. 975–986, 2009.
- [30] T. Melamed, "TE and TM beam decomposition of time-harmonic electromagnetic waves," *J. Opt. Soc. Am. A*, vol. 28, pp. 401–409, 2011.
- [31] T. Melamed, "Pulsed beam expansion of electromagnetic aperture fields," *Progr. Electromagn. Res.*, vol. PIER 114, pp. 317–332, 2011.
- [32] D. J. Hoppe and Y. Rahmat-Samii, "Gaussian beam reflection at a dielectric-chiral interface," *J. Electromag. Waves Appl.*, vol. 6, pp. 603–624, 1992.
- [33] R. Ianconescu and E. Heyman, "Pulsed beam diffraction by a perfectly conducting wedge. Exact solution," *IEEE Trans. Antennas Propag.*, vol. 42, pp. 1377–1385, 1994.
- [34] E. Heyman and R. Ianconescu, "Pulsed beam diffraction by a perfectly conducting wedge. Local scattering models," *IEEE Trans. Antennas Propag.*, vol. 43, pp. 519–528, 1995.
- [35] O. Pascal, F. Lemaitre, and G. Soum, "Paraxial approximation effect on a dielectric interface analysis," *Ann. Telecommun.*, vol. 51, pp. 206–218, 1996.
- [36] O. Pascal, F. Lemaitre, and G. Soum, "Dielectric lens analysis using vectorial multimodal Gaussian beam expansion," *Ann. Telecommun.*, vol. 52, pp. 519–528, 1997.
- [37] W. B. Dou and E. K. N. Yung, "Diffraction of an electromagnetic beam by planar structures," *J. Electromag. Waves Appl.*, vol. 15, pp. 1539–1549, 2001.
- [38] H. Sakurai and S. Kozaki, "Scattering of a Gaussian beam by a radially inhomogeneous dielectric sphere," *J. Electromag. Waves Appl.*, vol. 15, pp. 1673–1693, 2001.

- [39] H. T. Anastassiou and P. H. Pathak, "Closed form solution for three-dimensional reflection of an arbitrary Gaussian beam by a smooth surface," *Radio Science*, vol. 37, pp. 1–8, 2002.
- [40] M. Katsav and E. Heyman, "A beam summation representation for 3-D radiation from a line source distribution," *IEEE Trans. Antennas Propag.*, vol. 56, pp. 602–605, 2008.
- [41] M. Katsav and E. Heyman, "Gaussian beams summation representation of half plane diffraction: A full 3-D formulation," *IEEE Trans. Antennas Propag.*, vol. 57, pp. 1081–1094, 2009.
- [42] Y. Hadad and T. Melamed, "Non-orthogonal domain parabolic equation and its Gaussian beam solutions," *IEEE Trans. Antennas Propag.*, vol. 58, pp. 1164–1172, 2010.
- [43] Y. Hadad and T. Melamed, "Parameterization of the tilted Gaussian beam waveobjects," *Progr. Electromagn. Res.*, vol. PIER 102, pp. 65–80, 2010.
- [44] E. Heyman and T. Melamed, "Certain considerations in aperture synthesis of ultrawideband/short-pulse radiation," *IEEE Trans. Antennas Propag.*, vol. 42, pp. 518–525, 1994.
- [45] E. Heyman and T. Melamed, "Space-time representation of ultra wide-band signals," in *Advances in Imaging and Electron Physics*. The Netherlands: Elsevier, 1998, vol. 103, pp. 1–63.
- [46] T. Melamed, "Time-domain phase-space Green's functions for inhomogeneous media," in *Ultrawideband/Short Pulse Electromagnetics 6*, E. L. Mokole, M. Kragalott, K. R. Gerlach, M. Kragalott, and K. R. Gerlach, Eds. New York: Springer-Verlag, 2007, pp. 56–63.
- [47] G. Gordon, E. Heyman, and R. Mazar, "A phase-space Gaussian beam summation representation of rough surface scattering," *J. Acoust. Soc. Am.*, vol. 117, pp. 1911–1921, 2005.
- [48] G. Gordon, E. Heyman, and R. Mazar, "Phase space beam summation analysis of rough surface waveguide," *J. Acoust. Soc. Am.*, vol. 117, pp. 1922–1932, 2005.



Yakir Hadad was born in Beer Sheva, Israel, in 1984. He received the B.Sc. (*summa cum laude*) and M.Sc. (*summa cum laude*) degrees in electrical and computer engineering from Ben-Gurion University of the Negev, Israel, in 2005 and 2008, respectively.

Currently, he is a Ph.D. student at the Department of Physical-Electronics, School of Electrical Engineering, Tel-Aviv University, Israel. His main fields of interest are asymptotic methods, artificial materials and analytic modeling in electromagnetics.



Timor Melamed was born in Tel-Aviv, Israel, in January 1964. He received the B.Sc. degree (*magna cum laude*) in electrical engineering in 1989 and the Ph.D. degree in 1997, both from Tel-Aviv University.

From 1996 to 1998, he held a postdoctoral position at the Department of Aerospace and Mechanical Engineering, Boston University. Currently, he is with the Department of Electrical and Computer Engineering, Ben-Gurion University of the Negev, Israel. His main fields of interest are analytic techniques in wave theory, transient wave phenomena,

inverse scattering and electrodynamics.